Acta Ophthalmologica

ACTA OPHTHALMOLOGICA 2022

Reliability analysis of successive Corneal Visualization Scheimpflug Technology measurements in different keratoconus stages

Elias Flockerzi,[1] Larissa Häfner,[1] Kassandra Xanthopoulou,[1] Loay Daas,[1] Cristian Munteanu,[1] Achim Langenbucher[2] and Berthold Seitz[1]

[1]Department of Ophthalmology, Saarland University Medical Center, Homburg, Germany
[2]Department of Experimental Ophthalmology, Saarland University Medical Center, Homburg, Germany

ABSTRACT.

Background: **This study assesses the reliability of successive corneal biomechanical response measurements by the Corneal Visualization Scheimpflug Technology (CST, Corvis ST®, Oculus Optikgeräte, Wetzlar, Germany) in different keratoconus (KC) stages.**

Methods: **A total of 173 eyes (15 controls: 15 eyes, and 112 KC patients: stages 1|1–2|2|2–3|3|3–4|4, *n* = 26|16|36|18|31|26|5 according to Topographical KC Classification, TKC) were repeatedly examined five times with the CST, each after repositioning the patient's head and re-adjusting the device. Tomographical analysis (Pentacam HR®; Oculus, Wetzlar, Germany) was performed once before and once after CST measurements. Outcome measures included (1) A1 velocity, (2) deformation amplitude (DA) ratio 2 mm, (3) integrated radius, (4) stiffness parameter A1 and (5) Ambrósio relational thickness to the horizontal profile (ARTh). The Corvis Biomechanical Index (CBI) is reported to be extracted out of these parameters. Mean values of the five measurements and Cronbach's α were calculated as a measure for reliability.**

Results: **Ambrósio relational thickness to the horizontal profile and SPA1 were significantly higher in controls (534|123) compared to TKC1 (384|88), TKC2 (232|66), TKC3 (152|55) and TKC4 (71|27; p < 0.0001). The other parameters were similar in controls and TKC1 (A1 velocity: 0.148|0.151 m/s; integrated radius: 8.2|8.6 mm^{-1}), but significantly higher in TKC stages 2 to 4 (DA ratio 2 mm: 5.5|6.3|8.0; A1 velocity: 0.173|0.174|0.186 m/second; integrated radius: 10.9|12.8|19.0 mm^{-1}; p < 0.0001). All parameters proved to be highly reliable (Cronbach's α ≥ 0.834) and the corneal tomography remained unaffected.**

Conclusions: **The individual parameters included in the CBI (consisting of ARTh, SPA1, DA ratio 2 mm, A1 velocity and integrated radius) are highly reliable but differ KC stage-dependently.**

Key words: cornea – corvis ST – dynamic corneal response – ectasia – keratoconus – reliability

Acta Ophthalmol. 2022: 100: e83–e90

doi: 10.1111/aos.14857

Introduction

Keratoconus (KC) is characterized by a bilateral asymmetric progressive thinning of the cornea resulting in irregular astigmatism and visual impairment (Goebels et al. 2015). The diagnosis of early KC forms is crucial as the disease can be stabilized by corneal crosslinking (Wollensak et al. 2003). The same applies for the evaluation for refractive surgery as KC represents a contraindication. The diagnosis is usually based upon Placido-based corneal topography (Goebels et al. 2013) or Scheimpflug tomographic imaging (Belin & Ambrósio 2013; Belin 2020; Flockerzi et al. 2020a,b) and biomechanical analysis of the cornea (Elham et al. 2017; Langenbucher et al. 2020).

The Corneal Visualization Scheimpflug Technology (Corvis ST® (CST); Oculus, Wetzlar, Germany) enables KC detection based on corneal biomechanics and Dynamic Corneal Response (DCR) parameters. The CST utilizes an ultra-high-speed Scheimpflug camera combined with a non-contact tonometer. After a standardized air puff indentation, it visualizes and measures the corneal deformation response (Vinciguerra et al. 2016; Ambrósio et al. 2017).

The Corvis Biomechanical Index (CBI) combines different biomechanical parameters to distinguish between KC and healthy corneae (Reisdorf 2019). These include (1) the speed of the corneal apex at the inward applanation A1 (A1 velocity), (2) the ratio between the central deformation and the average 2 mm on either side of the centre (DA ratio 2 mm), (3) the integrated sum of the reciprocal of the radius between the inward and outward applanation (integrated radius), (4) the resultant pressure at inward applanation A1 divided by corneal displacement in comparison with the undeformed cornea (SP-A1) and (5) the thinnest corneal point in relation to the pachymetric progression indices Ambrósio relational thickness through the horizontal meridian (ARTh).

Whilst the reliability of successive Scheimpflug imaging and anterior segment optical coherence tomography measurements decreases with increasing KC severity (Flockerzi et al.2021), the two first CST reliability studies in KC patients found the CST measurements in keratoconic eyes to be repeatable and reproducible based on three measurements per eye (Yang et al. 2019; Herber et al. 2020). Whereas those studies summarized several KC stages in groups, the aim of the current study was to analyse the reliability of the CST measurements in each KC stage based on the Topographical KC Classification (TKC) and five successive measurements per eye. Since each CST measurement also involves a mechanical impulse on the cornea, the current study includes a comparison of corneal tomography values before and after the CST measurements.

Methods

A total of 158 corneae of 112 patients with different KC stages (1 (n = 26), 1–2 (n = 16), 2 (n = 36), 2–3 (n = 18), 3 (n = 31), 3–4 (n = 26), 4 (n = 5)), according to the Topographical KC Classification (TKC) provided by Pentacam software, were chosen from the Homburg Keratoconus Center HKC (Goebels et al. 2013; Flockerzi et al. 2020b). Since Belin's ABCD KC classification (Belin et al. 2015; Belin & Duncan 2016) includes posterior corneal curvature analysis and therefore provides a more precise KC classification than TKC, the corneae included in this study were also classified according to this classification (Fig. 1). Keratoconus was diagnosed (1) based on clinical slit lamp findings (paracentral corneal thinning and steepening, Vogt Striae, Fleischer ring, scar formation), (2) posterior elevation at the thinnest point ≥ 13 μm (based on a 8 mm reference sphere), (3) a thinnest corneal thickness < 580 μm and (4) a spherical equivalent < 0 (myopic)(Belin 2020).

The control group consisted of 15 corneae of 15 healthy subjects. The patients were older than 18 years, did not have any corneal surgery in their history and stopped wearing contact lenses at least three days prior to the measurements. Patients with diabetes mellitus were excluded. The study (trial number NCT03923101, U.S. National Institutes of Health, ClinicalTrials.gov) adhered to the principles of the Declaration of Helsinki and was approved by the local ethics committee of Saarland (Ethikkommission bei der Ärztekammer des Saarlandes, approval number 121/20).

All subjects provided written consent to participate in this study. Every eye was examined (1) with the Scheimpflug tomograph Pentacam HR® (Oculus, Wetzlar, Germany), then (2) with five successive measurements by the Corvis ST® and (3) again with the Pentacam HR® during one visit by the same experienced examiner (LH). The patients were able to fixate on the fixation target displayed within the device. The Pentacam HR® and CST measurements were conducted during regular follow-up examinations between 09.00 am and 04.00 pm to avoid diurnal anterior segment changes (Read & Collins 2009). The patients were asked to blink prior to the measurements with the intention to achieve a regular tear film distribution on the cornea. They were asked to keep their eyes wide open during the measurements. After each measurement, the patients sat back and had one minute to recover before their head was readjusted on the chinrest of the device prior to the next measurement. Both devices were used in automatic release mode whenever possible, but some abnormally deformed corneae required switching to manual release mode.

In controls and early KC stages, only measurements with a quality score 'OK' were included. However, restrictions regarding the quality score had to be accepted in advanced KC stages (TKC3-4 and TKC4), as they do go along with 'model deviations' by definition.

The CST outcome measures consisted of the five DCR parameters included in the CBI: (1) A1 velocity, (2) deformation amplitude (DA) ratio 2 mm, (3) integrated radius, (4) stiffness parameter A1 (SP-A1) and (5) Ambrósio relational thickness to the horizontal profile (ARTh). A combination of the CBI and Pentacam-derived Scheimpflug tomographic data leads to the tomographic biomechanical index (TBI) calculated by the CST software (Ambrósio et al. 2017), which was also assessed.

The comparison of corneal tomography before and after the CST measurements was carried out based on the

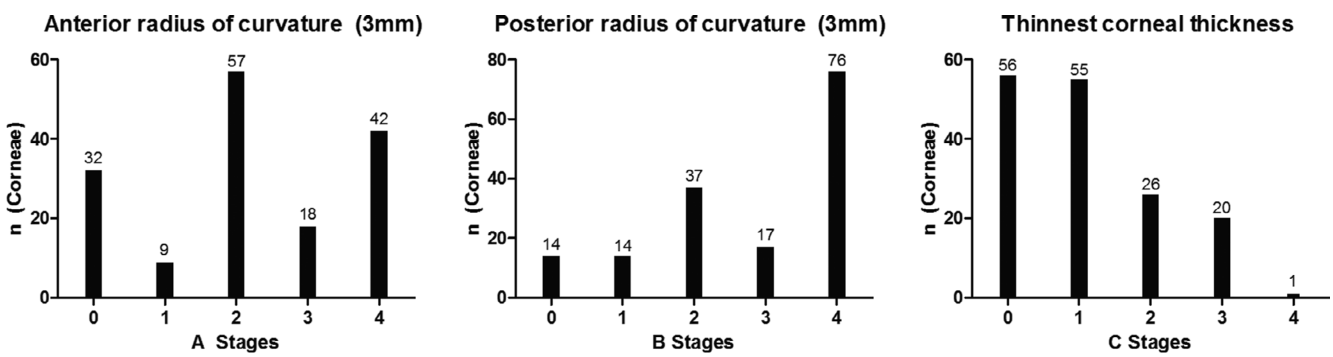

Fig. 1. A–C, KC severity distribution in this study: A (anterior radius of curvature) stages 0–4, B (posterior radius of curvature) stages 0–4, C (thinnest corneal thickness) stages 0–4, total: 158 KC corneae.

Wilcoxon matched pairs test and the following tomographic parameters: K1, K2, Kmean (calculated at a 3 mm diameter position) and astigmatism for anterior and posterior corneal curvature, the pachymetry at the apex and thinnest corneal thickness as well as the KC indices included in the Pentacam software.

Cronbach's alpha was calculated to prove the TKC stage-dependent reliability of the CST measurements. Calculations and figure drafts were done using SPSS software (version 20.0; International Business Machines Corporation, Armonk, NY, USA).

Results

This study included 158 KC corneae of 112 patients (77 right eyes and 81 left eyes) and 15 healthy corneae from 15 controls (eight right eyes and seven left eyes). The controls were all classified as stage A0|B0|C0 according to Belin and Duncan's ABCD classification (Belin et al. 2015; Belin & Duncan 2016). The mean age was 39.0 ± 13.8 years in the KC group and 34.0 ± 14.9 years in the control group. In the KC group, the most frequent anterior parameter was A2 followed by A4 > A0>A3 > A1 (Fig. 1). The posterior parameter distribution was B4 > B2>B3 > B1=B0 and the thinnest corneal thickness ('C') was C0 > C1>C2 > C3>C4 (Fig. 1). The mean Belin/Ambrósio Enhanced Ectasia total deviation index (BAD-D) score was 9.77 ± 6.5 and the mean thinnest corneal thickness was 471 ± 55.6 in the KC group. Therefore, this study covers a wide spectrum of KC severity according to both the TKC and ABCD classification.

The KC stage dependent changes of the DCR parameters were analysed. A1 velocity, DA ratio 2 mm and integrated radius increased from TKC1 to TKC4 (Figs 2 and 3, Tables 1 and 2). Stiffness parameter A1 and ARTh decreased from TKC1 to TKC4 (Figs 2 and 3). A significant difference between TKC1 and the control group was detected for DA ratio 2 mm, SP-A1 and ARTh (Tables 1 and 2). The values of the DCR parameters DA ratio 2 mm, integrated radius, SP-A1 and ARTh showed significant differences between all TKC main groups (TKC1 to TKC2, TKC2 to TKC3, TKC3 to TKC4, $p < 0.01$, Tables 1 and 2). The analysis was carried out based on the analysis of variances (anova) with Bonferroni correction.

The CBI showed a wide range of values in the stages TKC1 and TKC1-2 (Fig. 2). Starting from stage TKC2 onwards, the scattering of the values decreased and most KC were detected with a pathological CBI of approximately 1 (Fig. 2). The TBI that includes biomechanical and tomographic data was close to 0 in the control group (0.08 ± 0.13) and close to 1 (≥0.94 ± 0.17) in all TKC stages (Table 1).

The reliability of the DCR parameter measurements was analysed based on Cronbach's alpha, which was calculated for each DCR parameter in the control group and in each KC stage (Table 3). The smallest value for Cronbach's alpha was 0.834 revealing excellent reliability of the DCR parameter measurements (Table 3).

The Pentacam tomography measurements before and after the series of five successive CST measurements were compared based on the Wilcoxon matched pairs test, which revealed that there was no significant difference between both measurements apart from a few single parameters (Table 4).

Discussion

Besides corneal tomography, the analysis of corneal biomechanics facilitates the early diagnosis of KC because a biomechanical corneal destabilization with abnormal CST measurements can precede tomographic abnormalities (Ambrósio et al. 2017; Elham et al. 2017). Prior to the application and interpretation of the DCR parameters at different KC stages, the behaviour of the different biomechanical parameters and the reliability of their measurement depending on KC stage should be analysed.

The current study therefore investigated (1) the KC stage dependent characteristics of corneal biomechanics, (2) the reliability of the biomechanical parameters summarized within the CBI and (3) the influence of repeated mechanical stress in form of repeated CST measurements on the reproducibility of corneal tomography measurements.

Several studies reported that A1 velocity, DA ratio 2 mm and integrated radius were found to be significantly higher in KC groups of mixed stages than in healthy corneae. A1 velocity ranged from 0.15 to 0.17 m/s in healthy corneae (Lopes et al. 2017; Miki et al. 2017) and 0.17–0.2 m/s in KC corneae (Roberts et al. 2017; Chan et al. 2018). For DA ratio 2 mm, the reported values in healthy corneae range from 4.29 (Lopes et al. 2017) to 4.55 with a significantly higher value of 6.6 in a KC group of mixed stages (Chan et al. 2018). The parameter integrated radius was also reported to be significantly higher in a KC group with different included stages in comparison with healthy controls (Yang et al. 2019). In contrast, the parameters SP-A1 and ARTh were reported to show smaller values in KC than in healthy corneae (Roberts et al. 2017; Yang et al. 2019).

The current study demonstrated that mean A1 velocity, DA ratio 2 mm and integrated radius increased significantly according to the main TKC stages (Figs 2 and 3, Tables 1 and 2). The values for SP-A1 and ARTh decreased signficantly according to the main TKC stages (Figs 2 and 3, Tables 1 and 2). Based on those findings, this study traces the changes of the corneal DCR parameters in dependence of all TKC stages.

Biomechanical analysis of the human cornea has shown that the deformation amplitude after an air puff indentation is greater in KC than in healthy corneae (Ali et al. 2014). This decreased resistance to deformation has been attributed to a reduced corneal volume going along with alterated proteoglycan content, reduced keratocyte and (Ali et al. 2014) nerve fibre density (Flockerzi et al. 2020a), less collagen lamellae (Chan et al. 2018) and endothelial alterations (Goebels et al. 2018). Thus, the greater deformation in KC is characterized by an increased velocity after applanation (A1 velocity), a greater difference between the deformation within the centre and defined paracentral regions (DA ratio 2 mm), the greater maximal value of inverse radius of curvature during the concave phase of the deformation (integrated radius, Chan et al. 2018), a reduced stiffness (SP-A1) and is due to a thinned cornea (ARTh, Vinciguerra et al. 2016).

The CBI is reported to include the five aforementioned DCR parameters and its value approaches 0 in a healthy cornea and 1 in KC (Vinciguerra et al. 2016). The

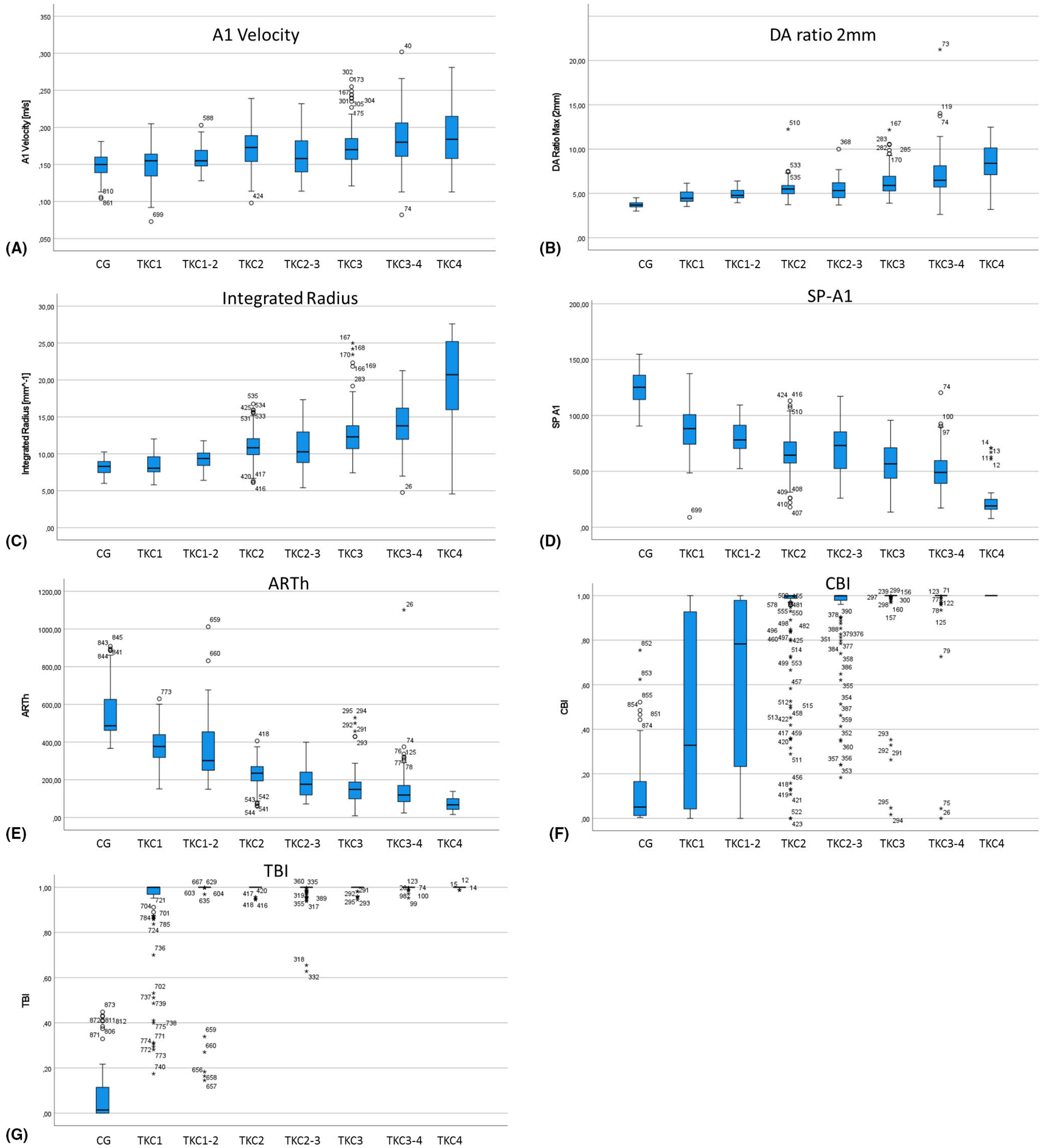

Fig. 2. A–G, Boxes with medians, 25th and 75th percentiles; whiskers representing the range of all values for (A) A1 velocity, (B) deformation amplitude (DA) ratio 2 mm, (C) integrated radius, (D) stiffness parameter A1 (SP-A1), (E) Ambrósio relational thickness to the horizontal profile (ARTh), (F) Corvis Biomechanical Index (CBI) and (G) Tomographic Biomechanical Index (TBI) according to Topographical KC Classification (TKC) stage; CG, control group.

CBI was close to 0 in the control group (mean ± SD, 0.12 ± 0.16) and close to 1 in TKC2 (0.92 ± 0.21), TKC3 (0.97 ± 0.14) and TKC4 (1.0 ± 0.0, Table 1, Figs 2 and 3). However, TKC1 and TKC1-2 showed a wider spreading of values (mean ± SD: 0.46 ± 0.4 (TKC1) and 0.62 ± 0.39 (TKC1-2, Table 1, Figs 2 and 3)), which makes the binary decision system of the CBI less informative for these KC stages. The wider spreading of the CBI values in early KC stages could be due to the fact that the DCR parameters the CBI is based on correlate with corneal thickness (Vinciguerra et al. 2016). Therefore, borderline results can be expected in early or subclinical KC stages, making the CBI less suitable for screening patients for crosslinking or refractive surgery. It might be for that reason that subclinical

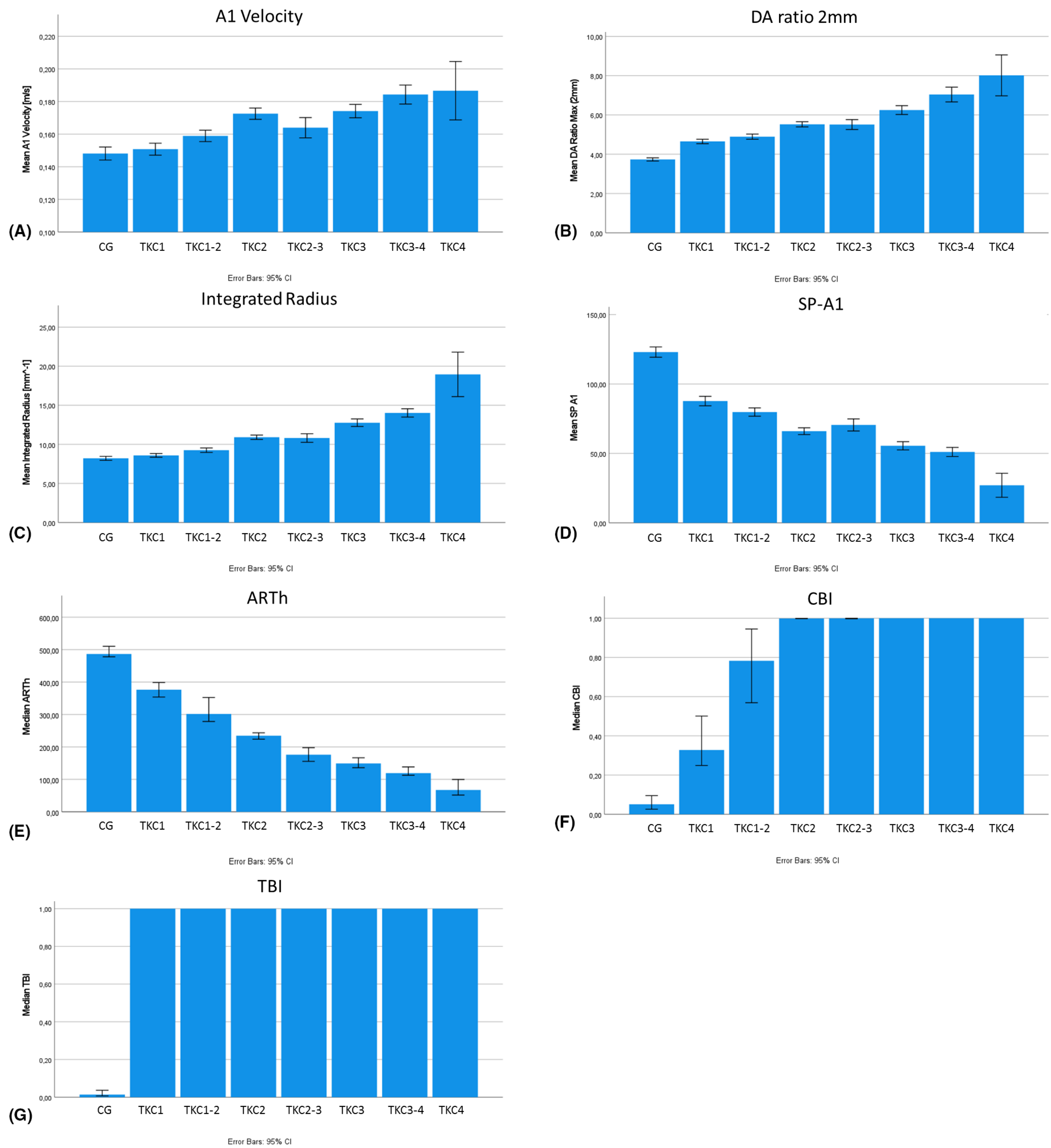

Fig. 3. A–D, mean with 95% confidence intervals in controls (CG) and TKC1 to TKC4 for (A) A1 velocity, (B) deformation amplitude (DA) ratio 2 mm, (C) integrated radius and (D) stiffness parameter A1 (SP-A1). E–G, median with 95% confidence intervals in controls (CG) and TKC1 to TKC 4 for (E) Ambrósio relational thickness to the horizontal profile (ARTh), (F) Corvis Biomechanical Index (CBI) and Tomographic Biomechanical Index (TBI) as the values were not normally distributed.

KC forms were excluded in the publication introducing the CBI (Vinciguerra et al. 2016). As the CBI is based on biomechanical data only, the TBI is more suitable in these early stages as it adds tomographic data to the biomechanical data. It combines the CBI with tomographic data derived from the Pentacam to ensure better detection of early KC forms: The TBI was close to 0 in the control group and close to 1 in all TKC stages (Table 1), which indicates a good separation between healthy and KC corneae.

In order to distinguish a KC from a healthy cornea with 100% sensitivity and 100% specificity based on tomographic data, it requires a Belin/Ambrósio Enhanced Ectasia total deviation index (BAD-D) score of more than 2.1 (Muftuoglu et al. 2015). In this

Table 1. Mean ± SD for dynamic corneal response parameters in the control group (CG) and TKC1-4.

TKC	CG	1	2	3	4
A1v (m/s)	0.148 ± 0.017	0.151 ± 0.022	0.173 ± 0.023	0.174 ± 0.026	0.186 ± 0.043
DAr2mm	3.74 ± 0.35	4.65 ± 0.65	5.53 ± 0.90	6.26 ± 1.41	8.02 ± 2.53
IR	8.2 ± 1.1	8.6 ± 1.4	10.9 ± 1.9	12.8 ± 3.0	19.0 ± 6.9
SP-A1	122.9 ± 16.1	87.7 ± 20.1	65.7 ± 16.4	55.3 ± 18.5	27.0 ± 20.9
ARTh	535.3 ± 131.6	383.5 ± 105.9	231.5 ± 71.4	152.4 ± 84.6	70.8 ± 39.3
CBI	0.12 ± 0.16	0.46 ± 0.40	0.92 ± 0.21	0.97 ± 0.14	1.0 ± 0.0
TBI	0.08 ± 0.13	0.94 ± 0.17	0.99 ± 0.01	1.00 ± 0.01	1.00 ± 0.01

A1v = A1velocity; ARTh = Ambrósio relational thickness to the horizontal profile; CBI = Corvis Biomechanical Index; DAr2mm = deformation amplitude (DA) ratio 2 mm; IR = integrated radius; SP-A1 = stiffness parameter A1; TBI = Tomographic Biomechanical Index.

Table 2. P-values calculated by anova with Bonferroni correction.

	A1 velocity	DA ratio 2 mm	Integrated radius	SP-A1	ARTh
CG-TKC1	1.0	<0.0001	0.6	<0.0001	<0.0001
TKC1-TKC1-2	0.559	1.0	1.0	0.043	0.405
TKC1-TKC2	<0.0001	<0.0001	<0.0001	<0.0001	<0.0001
TKC2-TKC2-3	0.23	1.0	1.0	1.0	0.135
TKC2-3	1.0	<0.0001	<0.0001	<0.0001	<0.0001
TKC3-TKC3-4	0.021	<0.0001	0.001	1.0	1.0
TKC3-TKC4	0.61	<0.0001	<0.0001	<0.0001	0.012
TKC3-4-TKC4	1.0	0.009	<0.0001	<0.0001	0.048

Significant differences between all TKC main groups (TKC1 versus TKC2, TKC2 versus TKC3, TKC3 versus TKC4) for deformation amplitude (DA) ratio 2mm, integrated radius, stiffness parameter A1 (SP-A1) and Ambrósio relational thickness to the horizontal profile (ARTh).

Table 3. Reliability statistics based on Cronbach's alpha.

Reliability – Cronbach's alpha					
TKC	A1 velocity	DA ratio 2 mm	Integrated radius	SP-A1	ARTh
CG	0.927	0.977	0.990	0.966	0.991
1	0.951	0.982	0.968	0.960	0.979
1-2	0.958	0.982	0.965	0.979	0.970
2	0.959	0.881	0.933	0.977	0.984
2-3	0.980	0.940	0.971	0.961	0.987
3	0.959	0.979	0.992	0.981	0.992
3-4	0.914	0.834	0.948	0.979	0.872
4	0.952	0.920	0.985	0.995	0.939

Excellent reliability of all measurements (Cronbach's alpha ≥ 0.834) independent of KC stage.
TKC = Topographical KC Classification, CG = control group, DA ratio 2mm = deformation amplitude (DA) ratio 2mm, SP-A1 = stiffness parameter A1, ARTh = Ambrósio relational thickness to the horizontal profile.

study, the mean BAD-D score was 9.77 ± 6.5 (mean ± SD) in the KC group and therefore, the CBI values in TKC1 and TKC1-2 cannot be attributed to the inclusion of subclinical or form fruste KC.

Considering the reliability of successive CST measurements, one study including 48 (Miki et al. 2017) and another including 32 healthy corneae (Lopes et al. 2017) found good repeatability and reliability in most parameters measured by the CST. Yang et al. analysed the reliability of three successive CST measurements in 77 healthy and 77 mild to moderate KC corneae (Yang et al. 2019). Although one could hypothesize that the reliability of successive CST measurements decreases with increasing KC severity as it was proven for successive Scheimpflug imaging and anterior segment optical coherence tomography measurements in KC (Flockerzi et al. 2021), the conclusion was that there was an excellent reliability also for the KC group (Cronbach's alpha > 0.87, Yang et al. 2019). Herber et al. divided a collective of 98 KC corneae in three groups according to KC severity (mean BAD-D 6.6 ± 3.3) and performed a reliability analysis, which led to the result that the DCR parameters measured by the CST were of excellent reliability (Herber et al. 2020).

The current study evaluated the reliability of successive CST measurements separately in each TKC stage based on 158 KC corneae with the aim to cover the full spectrum of KC severity (mean BAD-D 9.77 ± 6.5). Main outcome measures were the DCR parameters that form the CBI which turned out to have an excellent reliability in every TKC stage (Cronbach's alpha ≥ 0.834, Table 3).

A Pentacam-based corneal tomography was performed prior to the CST measurements for classification into the respective TKC stages. It was reported that the corneal apex is exposed to a maximum air pressure of 95 mmHg during a CST measurement (Eliasy et al. 2019), which represents mechanical stress to the cornea. The tomography was repeated after the series of CST measurements and both tomographies were compared for each cornea using the Wilcoxon matched pairs test. The finding that there were no significant differences between the respective tomographic measurements before and after the CST measurements, apart from two single values (TCT in the control group and K2F in TKC1, Table 4) and fluctuations in the KC

Table 4. Mean ± SD for tomographic parameters (1) before and (2) after the series of five successive CST measurements.

	Controls	TKC1	TKC1-2	TKC2	TKC2-3	TKC3	TKC3-4	TKC4
K1F (1)	43.0 ± 1.1	43.6 ± 1.6	44.2 ± 1.8	45.7 ± 2.4	46.1 ± 3.4	49.5 ± 4.2	52.6 ± 5.9	61.1 ± 11.0
K1F (2)	43.0 ± 1.1	43.6 ± 1.6	44.2 ± 1.7	45.7 ± 2.4	46.0 ± 3.7	49.5 ± 4.2	52.4 ± 5.8	59.1 ± 13.7
p	0.3	0.9581	0.6665	0.0646	0.432	0.3759	0.2467	0.1875
K2F (1)	43.9 ± 1.1	45.9 ± 1.8	46.4 ± 2.2	49.0 ± 2.5	49.5 ± 3.6	52.8 ± 5.1	55.9 ± 7.0	68.1 ± 14.1
K2F (2)	43.9 ± 1.1	45.8 ± 1.8	46.4 ± 2.2	49.0 ± 2.6	49.5 ± 3.6	52.9 ± 5.1	55.9 ± 7.0	67.7 ± 15.0
p	1.0	***0.0126***	0.6066	0.8377	0.6523	0.478	0.9203	0.6845
KmF (1)	43.4 ± 1.1	44.7 ± 1.7	45.2 ± 1.9	47.3 ± 2.3	47.7 ± 3.4	51.1 ± 4.6	54.2 ± 6.3	64.3 ± 11.8
KmF (2)	43.4 ± 1.1	44.7 ± 1.7	45.3 ± 1.9	47.3 ± 2.4	47.7 ± 3.6	5.1 ± 4.6	54.1 ± 6.3	63.0 ± 14.0
p	0.59	0.3423	0.6643	0.684	0.5694	0.8758	0.2229	0.1875
AstigF (1)	0.9 ± 0.5	2.3 ± 1.0	2.2 ± 1.2	3.4 ± 1.6	3.5 ± 1.7	3.3 ± 1.6	3.3 ± 2.4	7.1 ± 7.7
AstigF (2)	0.9 ± 0.5	2.3 ± 0.9	2.3 ± 1.3	3.2 ± 1.5	3.4 ± 1.6	3.4 ± 1.7	3.5 ± 2.5	8.7 ± 5.8
p	0.4485	0.4984	0.5072	0.2092	0.7223	0.5099	0.2398	0.3125
K1B (1)	−6.1 ± 0.2	−6.2 ± 0.3	−6.4 ± 0.4	−6.8 ± 0.6	−6.7 ± 0.7	−7.5 ± 0.9	−8.0 ± 1.1	−9.5 ± 2.4
K1B (2)	−6.1 ± 0.2	−6.2 ± 0.4	−6.4 ± 0.4	−6.7 ± 0.6	−6.7 ± 0.7	−7.5 ± 0.9	−8.0 ± 1.1	−9.1 ± 3.2
p	0.3458	0.4541	0.5898	0.8274	0.7513	0.974	0.6943	0.625
K2B (1)	−6.4 ± 0.2	−6.8 ± 0.4	−6.9 ± 0.5	−7.5 ± 0.7	−7.3 ± 0.7	−8.2 ± 1.1	−8.7 ± 1.3	−10.9 ± 2.6
K2B (2)	−6.4 ± 0.2	−6.8 ± 0.4	−6.9 ± 0.5	−7.5 ± 0.7	−7.4 ± 0.7	−8.2 ± 1.1	−8.7 ± 1.3	−10.9 ± 2.9
p	1.0	0.9343	0.1934	0.0975	0.7313	0.6487	1	0.8923
KmB (1)	−6.3 ± 0.2	−6.5 ± 0.3	−6.7 ± 0.4	−7.1 ± 0.6	−7.0 ± 0.6	−7.8 ± 1.0	−8.3 ± 1.2	−10.2 ± 2.5
KmB (2)	−6.3 ± 0.2	−6.5 ± 0.4	−6.6 ± 0.4	−7.1 ± 0.6	−7.0 ± 0.7	−7.8 ± 0.9	−8.3 ± 1.2	−9.9 ± 3.0
p	1.0	0.4374	0.0655	0.8272	0.8087	0.1071	0.6512	0.4375
AstigB (1)	0.3 ± 0.1	0.6 ± 0.2	0.5 ± 0.2	0.7 ± 0.3	0.6 ± 0.4	0.7 ± 0.5	0.6 ± 0.4	1.4 ± 0.9
AstigB (2)	0.3 ± 0.1	0.6 ± 0.2	0.5 ± 0.2	0.7 ± 0.4	0.6 ± 0.4	0.7 ± 0.4	0.7 ± 0.4	1.7 ± 1.1
p	0.3859	0.837	0.3437	0.4218	0.4587	0.9288	0.5895	0.375
PApex (1)	564 ± 42	530 ± 36	515 ± 32	488 ± 41	490 ± 41	459 ± 54	458 ± 51	384 ± 62
PApex (2)	566 ± 41	529 ± 37	514 ± 34	490 ± 41	488 ± 43	458 ± 55	461 ± 48.8	389 ± 80
p	**0.0347**	0.18	0.3473	0.1438	0.3423	0.7182	0.098	0.625
TCT (1)	561 ± 41	519 ± 41	506 ± 33	478 ± 43	474 ± 36	444 ± 56	444 ± 48	370 ± 54
TCT (2)	562 ± 42	517 ± 40	503 ± 35	475 ± 45	473 ± 39	443 ± 57	446 ± 44	362 ± 45
p	0.1276	0.0874	0.0908	0.9658	0.7942	0.5887	0.3885	0.3125
ISV (1)	16 ± 5.0	38 ± 5.3	51 ± 4.2	73 ± 9.0	92 ± 4.0	113 ± 7.7	154 ± 21	216 ± 6.1
ISV (2)	16 ± 4.3	37 ± 5.4	50 ± 5.5	75 ± 9.9	89 ± 7.0	112 ± 9.1	154 ± 20	208 ± 18
p	0.3053	***0.0178***	0.0679	0.1868	***0.0136***	0.2364	0.9899	0.4375
IVA (1)	0.1 ± 0.1	0.4 ± 0.1	0.6 ± 0.1	0.8 ± 0.2	1.0 ± 0.1	1.2 ± 0.2	1.6 ± 0.3	1.7 ± 0.8
IVA (2)	0.1 ± 0.0	0.4 ± 0.1	0.6 ± 0.1	0.8 ± 0.2	1.0 ± 0.2	1.2 ± 0.3	1.6 ± 0.3	1.7 ± 0.6
p	0.6558	0.2225	0.083	0.087	***0.0493***	0.5319	0.5719	0.8125
KI (1)	1.0 ± 0.0	1.1 ± 0.0	1.1 ± 0.0	1.2 ± 0.0	1.2 ± 0.1	1.3 ± 0.1	1.5 ± 0.1	1.7 ± 0.1
KI (2)	1.0 ± 0.0	1.1 ± 0.0	1.1 ± 0.0	1.2 ± 0.0	1.2 ± 0.1	1.3 ± 0.0	1.5 ± 0.1	1.6 ± 0.1
p	0.4070	***0.0106***	0.1851	0.0567	0.1413	0.9877	0.6711	1
CKI (1)	1.0 ± 0.0	1.0 ± 0.0	1.0 ± 0.0	1.0 ± 0.0	1.0 ± 0.0	1.1 ± 0.1	1.14 ± 0.1	1.2 ± 0.1
CKI (2)	1.0 ± 0.0	1.0 ± 0.0	1.0 ± 0.0	1.0 ± 0.0	1.0 ± 0.0	1.1 ± 0.1	1.13 ± 0.1	1.2 ± 0.1
p	0.7768	***0.0197***	0.3741	0.8271	0.2402	0.8039	***0.0238***	0.4982
IHA (1)	4.6 ± 3.7	21.7 ± 13	29.7 ± 20	37.9 ± 23	24.6 ± 15	31.0 ± 26.7	37.6 ± 24.6	64.0 ± 27.9
IHA (2)	5.2 ± 4.1	21.1 ± 13	21.5 ± 19	30.5 ± 25	27.2 ± 18	34.3 ± 28.0	28.7 ± 21	64.6 ± 47.1
p	0.1473	1	***0.0018***	***0.0411***	0.8276	0.55	0.134	1
IHD (1)	0.0 ± 0.0	0.0 ± 0.0	0.1 ± 0.0	0.1 ± 0.0	0.14 ± 0.0	0.2 ± 0.0	0.2 ± 0.0	0.3 ± 0.1
IHD (2)	0.0 ± 0.0	0.0 ± 0.0	0.1 ± 0.0	0.1 ± 0.0	0.13 ± 0.0	0.2 ± 0.0	0.3 ± 0.0	0.3 ± 0.1
p	0.3069	0.7329	0.1547	0.6381	***0.0085***	0.1612	0.2179	0.8125

p-Values calculated by Wilcoxon matched pairs test. Bold, significantly higher value after the CST measurements. Bold and italicized, significantly lower values after the CST measurements.

AstigB = astigmatism back, AstigF = astigmatism front, CKI = Central Keratoconus Index, IHA = Index of Height Asymmetry, IHD = Index of Height Decentration, ISV = Index of Surface Variance, IVA = Index of Vertical Asymmetry, K1B = K1 back, K1F = K1 front, K2B = K2 back, K2F = K2 front, KI = Keratoconus Index, KmB = Kmean back, KmF = Kmean front, PApex = Pachymetry at the Apex, TCT = Thinnest Corneal Thickness.

indices, confirms the excellent reliability of the CST measurements independent of KC stage.

A limitation of this study is the KC classification in stages according to the TKC classification. This classification is based on anterior topographic indices and does not include analysis of posterior corneal curvature. To compensate for this limitation, all corneae included in this study were re-classified according to the recent ABCD KC classification, which includes posterior corneal curvature analysis (Belin et al. 2015; Belin & Duncan 2016; Flockerzi et al.2020b ; Fig. 1). Both classifications prove, that a large number of different degrees of KC severity were included in this study.

The first conclusion of this study is that the DCR parameters included within the CBI differ significantly between the main TKC stages 1 to 4. Secondly, the five repeated CST measurements are of excellent reliability independent of TKC stage and thirdly, the mechanical stress on the cornea induced by the CST measurement does not influence the measurement of corneal tomography.

Finally, the Corvis ST® seems to be a highly reliable and promising device in the investigation of KC, which only in early TKC stages (TKC1 and TKC1-2) provides conspicuous but not clearly pathological CBI values. The TBI separates even more clearly between healthy and ectatic corneae at these early KC stages and should therefore be taken into account in daily use and practice.

References

Ali NQ, Patel DV & McGhee CNJ (2014): Biomechanical responses of healthy and keratoconic corneas measured using a non-contact scheimpflug-based tonometer. Invest Ophthalmol Vis Sci **55**: 3651–3659.

Ambrósio R, Lopes BT, Faria-Correia F et al. (2017): Integration of scheimpflug-based corneal tomography and biomechanical assessments for enhancing ectasia detection. J Refract Surg **33**: 434–443.

Belin MW (2020): Keratoconus and ectatic disease: evolving criteria for diagnosis. Klin Monbl Augenheilkd **237**: 740–744.

Belin M & Ambrósio R (2013): Scheimpflug imaging for keratoconus and ectatic disease. Indian J Ophthalmol **61**: 401.

Belin MW & Duncan JK (2016): Keratoconus: The ABCD Grading System. Klin Monbl Augenheilkd **233**: 701–707.

Belin MW, Duncan J, Ambrósio R & Gomes JAP (2015): A new tomographic method of staging / classifying keratoconus: The ABCD grading system. Int J Kerat Ect Cor Dis **4**: 85–93.

Chan TC, Wang YM, Yu M & Jhanji V (2018): Comparison of corneal dynamic parameters and tomographic measurements using Scheimpflug imaging in keratoconus. Br J Ophthalmol **102**: 42–47.

Elham R, Jafarzadehpur E, Hashemi H, Amanzadeh K, Shokrollahzadeh F, Yekta A & Khabazkhoob M (2017): Keratoconus diagnosis using Corvis ST measured biomechanical parameters. J Curr Ophthalmol **29**: 175–181.

Eliasy A, Chen K-J, Vinciguerra R et al. (2019): Determination of corneal biomechanical behavior in-vivo for healthy eyes using CorVis ST tonometry: stress-strain index. Front Bioeng Biotechnol **7**: 105.

Flockerzi E, Daas L & Seitz B (2020a): Structural changes in the corneal subbasal nerve plexus in keratoconus. Acta Ophthalmol **98**: e928–e932.

Flockerzi E, Elzer B, Daas L, Xanthopoulou K, Eppig T, Langenbucher A & Seitz B. (2021): The reliability of successive Scheimpflug imaging and anterior segment optical coherence tomography measurements decreases with increasing keratoconus severity. Cornea, [Epub ahead of print]

Flockerzi E, Xanthopoulou K, Goebels S et al. (2020b): Keratoconus staging by decades - a baseline ABCD classification of 1,000 patients in the Homburg Keratoconus Center (HKC). Br J Ophthalmol, [Epub ahead of print]

Goebels S, Eppig T, Seitz B, Szentmáry N, Cayless A & Langenbucher A (2018): Endothelial alterations in 712 keratoconus patients. Acta Ophthalmol **96**: e134–e139.

Goebels S, Eppig T, Wagenpfeil S, Cayless A, Seitz B & Langenbucher A (2015): Staging of keratoconus indices regarding tomography, topography, and biomechanical measurements. Am J Ophthalmol **159**: 733–738.e3.

Goebels S, Seitz B & Langenbucher A (2013): Diagnostics and stage-oriented therapy of keratoconus: introduction to the Homburg Keratoconus Center (HKC). Ophthalmologe **110**: 808–809.

Herber R, Vinciguerra R, Lopes B, Raiskup F, Pillunat LE, Vinciguerra P & Ambrósio R (2020): Repeatability and reproducibility of corneal deformation response parameters of dynamic ultra-high-speed Scheimpflug imaging in keratoconus. J Cataract Refract Surg **46**: 86–94.

Langenbucher A, Häfner L, Eppig T, Seitz B, Szentmáry N & Flockerzi E. (2020): Keratoconus detection and classification from parameters of the Corvis®ST : A study based on algorithms of machine learning. Ophthalmologe, [Epub ahead of print]

Lopes BT, Roberts CJ, Elsheikh A et al. (2017): Repeatability and reproducibility of intraocular pressure and dynamic corneal response parameters assessed by the corvis ST. J Ophthalmol **2017**: 8515742.

Miki A, Maeda N, Asai T, Ikuno Y & Nishida K (2017): Measurement repeatability of the dynamic Scheimpflug analyzer. Jpn J Ophthalmol **61**: 433–440.

Muftuoglu O, Ayar O, Hurmeric V, Orucoglu F & Kılıc I (2015): Comparison of multimetric D index with keratometric, pachymetric, and posterior elevation parameters in diagnosing subclinical keratoconus in fellow eyes of asymmetric keratoconus patients. J Cataract Refract Surg **41**: 557–565.

Read SA & Collins MJ (2009): Diurnal variation of corneal shape and thickness. Optom Vis Sci **86**: 170–180.

Reisdorf S (2019): Artificial intelligence for the development of screening parameters in the field of corneal biomechanics. Klin Monbl Augenheilkd **236**: 1423–1427.

Roberts CJ, Mahmoud AM, Bons JP, Hossain A, Elsheikh A, Vinciguerra R, Vinciguerra P & Ambrósio R (2017): Introduction of two novel stiffness parameters and interpretation of air puff-induced biomechanical deformation parameters with a dynamic scheimpflug analyzer. J Refract Surg **33**: 266–273.

Vinciguerra R, Ambrósio R, Elsheikh A, Roberts CJ, Lopes B, Morenghi E, Azzolini C & Vinciguerra P (2016): Detection of keratoconus with a new biomechanical index. J Refract Surg **32**: 803–810.

Wollensak G, Spoerl E & Seiler T (2003): Riboflavin/ultraviolet-a-induced collagen crosslinking for the treatment of keratoconus. Am J Ophthalmol **135**: 620–627.

Yang K, Xu L, Fan Q, Zhao D & Ren S (2019): Repeatability and comparison of new Corvis ST parameters in normal and keratoconus eyes. Sci Rep **9**: 15379.

Received on December 19th, 2020.
Accepted on March 2nd, 2021.

Correspondence:
Elias Flockerzi
Department of Ophthalmology
Saarland University Medical Center
66421 Homburg
Germany
Tel: 0049 6841 16-22302
Fax: 0049 6841 16-22479
Email: elias.flockerzi@uks.eu

We thank Mrs. Christina Turner for her valuable linguistic additions and corrections in this manuscript.

Financial Disclosures: Larissa Häfner, Kassandra Xanthopoulou, Loay Daas, Cristian Munteanu, Achim Langenbucher and Berthold Seitz declare that they don't have any financial disclosures in medicine. Elias Flockerzi has received a travel grant to the Second and Third Ophthalmology Cystinosis Forum (Orphan Europe, Ulm, Germany) and an invitation to a seminar on presentation training organized by the Santen GmbH (Munich, Germany).

All authors contributed to this work by providing their data, revising the manuscript, approving it for publication and agreeing to take full responsibility for all aspects of this work.